Materials Science & Engineering C 112 (2020) 110889

Contents lists available at ScienceDirect

Materials Science & Engineering C

journal homepage: www.elsevier.com/locate/msec

Synthesis of bio-mediated silver nanoparticles from *Silybum marianum* and their biological and clinical activities

Muzamil Shah[a], Sabir Nawaz[b], Hasnain Jan[a], Noor Uddin[c], Ashaq Ali[d], Sumaira Anjum[e], Nathalie Giglioli-Guivarc'h[f,g], Christophe Hano[g,h], Bilal Haider Abbasi[a,f,g,h,*]

[a] Department of Biotechnology, Quaid-i-Azam University, Islamabad 45320, Pakistan
[b] Department of Microbiology, Quaid-i-Azam University, Islamabad 45320, Pakistan
[c] Department of Chemistry, Quaid-i-Azam University, Islamabad 45320, Pakistan
[d] Key State Laboratory of Virology, Wuhan Institute of Virology, Chinese Academy of Sciences, 430072 Wuhan, China
[e] Department of Biotechnology, Kinnaird College for Women, Lahore 54000, Pakistan
[f] EA2106 Biomolécules et Biotechnologies Végétales, Université de Tours, 37000 Tours, France
[g] COSM'ACTIFS, Bioactifs et Cosmétiques, CNRS GDR3711, 45067 Orléans CEDEX 2, France
[h] Laboratoire de Biologie des Ligneux et des Grandes Cultures (LBLGC), INRA USC1328, Université d'Orléans, 45067 Orléans CEDEX 2, France

ARTICLE INFO

Keywords:
Silver nanoparticles
Green synthesis
Silybum
Antimicrobial
Anti-diabetic
Anti-inflammatory

ABSTRACT

The purpose of current study was green synthesis of silver nanoparticles (AgNPs) from seeds and wild *Silybum* plants in comparison with their respective extracts followed by characterization and biological potency. The biologically synthesized AgNPs were subjected to characterization using techniques like XRD, FTIR, TEM, HPLC and SPE. Highly crystalline and stable NPs were obtained using *Silybum* wild plant (NP1) and seeds (NP3) with size range between 18.12 and 13.20 nm respectively. The synthesized NPs and their respective extracts revealed a vast range of biological applications showing antibacterial, antioxidant, anti-inflammatory, cytotoxic and anti-aging potencies. The highest antioxidant activity (478.23 ± 1.9 μM, 176.91 ± 1.3 μM, 83.5 ± 1.6% μgAAE/mg, 156.32 ± 0.6 μgAAE/mg) for ABTS, FRAP, FRSA, TRP respectively was shown by seed extract (NP4) followed by highest value of (117.35 ± 0.9 μgAAE/mg) for TAC by wild extract (NP2). The highest antifungal activity (13 mm ± 0.76) against *Candida albicans* was shown by NP3 while antibacterial activity of (6 mm against *Klebsiella pneumonia*) was shown by NP3 and NP4. The highest anti-inflammatory activity (38.56 ± 1.29 against COX1) was shown by NP2. Similarly, the high value of (48.89 ± 1.34 against Pentosidine-Like AGEs) was shown by NP4. Also, the high anti-diabetic activity (38.74 ± 1.09 against α-amylase) was shown by NP4. The extracts and the synthesized NPs have shown activity against hepato-cellular carcinoma (HepG2) human cells. The HPLC analysis revealed that the highest value of silymarin component (silybin B 2289 mg/g DW) was found for NP4. Silydianin is responsible for capping. Among the green synthesized AgNPs and the extracts used, the effect of NP4 was most promising for further use.

1. Introduction

The word "nano" is derived from Greek, meaning extremely small or dwarf [1]. Nanotechnology is one of the emerged areas of science and technology that has changed the field of life sciences [2]. Nanoparticles can be defined as the materials having one dimension in nanometer range (1-100 nm) [3]. Nanotechnology has found its way in different areas like cosmetics [4], health care [5], food and feed [6], biomedical research [7], drug delivery [8], gene delivery [9], and environment [10]. Similarly, the nanotechnology has benefitted electronics, photo-chemistry and energy sciences [11]. Various physiochemical techniques like chemical reduction have been used for synthesis of AgNPs [12]. For the synthesis of metallic NPs, various approaches have been used, among which the greener route is considered ecofriendly method [13]. AgNPs synthesis by chemical reduction (sodium borohydride, ethylene glycol, hydrazine hydrate, etc) involves the absorption of chemicals on NPs surface, thus raising toxicity [14].

In order to formulate the NPs, biological route has received much more attention as compared to rest of the contemporary techniques (both physical and chemical) due to several important attributes like safety, environmental friendly protocols with non-toxic by products, gentle reaction condition requirements and the use of natural capping

* Corresponding author at: Department of Biotechnology, Quaid-i-Azam University, Islamabad 45320, Pakistan.
E-mail address: bhabbasi@qau.edu.pk (B.H. Abbasi).

https://doi.org/10.1016/j.msec.2020.110889
Received 24 November 2019; Received in revised form 11 March 2020; Accepted 20 March 2020
Available online 21 March 2020
0928-4931/

and reducing agents. The NPs thus produced through biological approach are comparatively stable and safer with much more diversity in terms of size and shape. Most abundantly used biological route for NPs synthesis is the use of plant extracts for formulation of ecofriendly NPs which cuts out the use of noxious chemicals with toxic effects. Plant mediated NPs synthesis results in formulation of NPs having definite shape and size. Currently, researchers are also working on the use of aqueous medium containing hydrolytic reagents for possible capping and stabilization of materials in nano-dimension.

Silver is known for having an inhibitory effect to many microorganisms and bacterial strains present in industrial and medical processes [15]. Silver products are familiar to have strong bactericidal and inhibitory effects, and wide spectrum antimicrobial properties [16], and these are practiced for centuries to care and prevent different diseases and infections [17]. AgNPs are used for anti-inflammatory, antifungal, antiplatelet and antiviral activity [18]. The AgNPs are less toxic to human cells compare silver ions [19]. In medicines, AgNPs and silver has various applications including creams and skin ointments containing silver to prevent open wounds and burns infection [20], implants and medical devices prepared with silver-embedded polymer [21]. Also the silver-impregnated fabrics are used in textile industry in sport equipment [22]. The antimicrobial covering and purification of drinking water based on materials surface coated with silver remove 99% pathogens [23]. Silver NPs were used with mPEGylated luteolin for selective visual detection of Hg^{2+} in water sample [24].

The anti-inflammatory activity of plant extract is usually assessed by measuring % of COX-2 (cyclooxygenase 2), COX-1 (cyclooxygenase 1), 15-LOX (15-lipoxygenase) and sPLA2 (secretory phospholipase A2). The endogenous enzymes, Cyclooxygenases (COXs) helps in maintaining tissue homeostasis of gastrointestinal tract, platelets, kidney and various types of cancers [25]. In inflammation process the COXs are the main players and key target for NSAIDs (non-steroidal anti-inflammatory drugs) development. COX-2 produces prostaglandin E2, the endogenous pain producing molecule, whereas COX-1 is the house keeping enzyme. The molecular mechanism of some anti-inflammatory drugs inhibits both COX-1 and COX-2 enzymes. So, the drugs which inhibit COX-2 and COX-1 enzymes cause adverse side effects like gastrointestinal bleeding and/or renal dysfunction. Thus, the researchers are seeking for better alternative that can inhibit expression of COX-2 only for drug development and discovery [26]. The current review on nutraceutical uses, pharmacological activities and chemistry of *Silybum* in liver diseases reported that silymarin, exhibited both immunomodulatory and anti-inflammatory potentials by deterring NF-κB pathway [27]. During inflammation process the compounds of plants inhibit these enzymes by acting as natural inhibitors [28].

The plants anti-aging activities are due to their key ability to minimize free radical damage to skin, with their ability to control enzyme activities involved in the process of aging. For instance, their ability to inhibit collagenase, hyaluronidase, or elastase involved in extracellular matrix components cleavage, or tyrosinase ability to activate SIRT1, a key regulator involved in both regulation of aging process and oxidative stress response, or inhibition of tyrosinase involves hyperpigmentation (skin aging) [29]. The effective enzymes inhibitors, pentacyclic triterpenoids are involved in cleavage of extracellular matrix components [30], while the phenolic acids are considered as possible potent activators of SIRT1 and strong antioxidants [31].

For biosynthesis of NPs the plants provide a better platform as they are nontoxic and provide natural capping agents as well. *Silybum marianum* consist of silymarin which is a mixture of complex polyphenolic molecules, including flavonolignans (silybin A, isosilybin A, silybin B, isosilybin B, isosilychristin, silychristin, silydianin) and a flavonoid (taxifolin) [32]. AgNPs have been biosynthesized from the leaf extract of *Capsicum annuum* and papaya fruit extract and their antimicrobial studies were reported [33]. The mechanism considered for plant mediated NPs synthesis is due to phytochemical presence. The responsible phytochemicals for ions reduction are terpenoids, flavonoids, quinones, carboxylic acids, amides, ketones and aldehydes [34]. Silymarin is nontoxic and can be used as safe herbal product unless inappropriate administration of therapeutic dosages [35]. The extract of *Silybum marianum* is used for AgNPs production through Keto-enol Tautomerization. The current study is designed to biosynthesize and characterize AgNPs from seeds (NP3) and wild *Silybum* (NP1) in comparison to their respective extracts (NP4 and NP2 respectively) and characterization of these silver NPs by XRD, UV–visible spectroscopy, HPLC and FTIR. Different biological assays like antioxidant, anti-inflammatory, anti-aging, and anti-diabetic were also performed. The HPLC of NPs and extracts are reported for the first time from *Silybum*.

2. Materials and methods

2.1. Reagents

Silver nitrate ($AgNO_3$) was purchased from Sigma Aldrich Company, Germany. *S. marianum* seeds and wild plants were obtained from, Quaid I Azam University Islamabad, Pakistan.

2.2. Biosynthesis of AgNPs from S. marianum

For the preparation of different extracts from dry seeds and wild plants, 20 g each were washed with distilled water several times for the dust removal purpose. The seeds were grinded while wild plants were cut into small pieces. Distilled water (200 mL) was added keeping extract to water ratio (*w/v*) of 1:10 respectively. After boiling for 2 h at 100 °C the extract was shifted to incubator for 24 h at 40 °C. The next day the extract was filtered and 1 mM $AgNO_3$ was added at the ratio of 1:5 (*v/v*) for seeds and 1:2 (v/v) for wild respectively. The mixture of plant extract and $AgNO_3$ solution was then kept in continuous light for 24 h after which, the absorbance was recorded through UV–Visible spectrophotometry. The reaction mixtures were kept at room temperature for 72 h and were monitored for complete reduction of all Ag ions into AgNPs. Once the synthesis of AgNPs was completed, the mixture was centrifuge in order to obtain AgNPs. For this purpose, the supernatant after centrifugation was discarded and the pellets (containing AgNPs) were washed thrice with distilled water and air dried.

3. Characterization

3.1. UV-spectroscopy

The purpose of UV–vis spectrophotometry was to observe the optical property of biologically synthesized AgNPs. AgNPs synthesis was monitored by mixing the plant extract and $AgNO_3$ solution (1 mM) in different ratios i.e. 1:1, 1:2, 1:10, 1:15 and 1:20 and the results were analyzed through UV–vis spectrophotometer (HALO DB-20S UV-VIS Double Beam, Australia) for highest peak and absorbance at zero and 24 h at room temperature between wavelength of 230 and 1100 nm.

The crystallinity and biosynthesis was confirmed using X-Ray Diffraction (XRD) (Model-D8 Advance, Bruker, Mannheim, Germany).

The size distribution and shape of the green synthesized silver NPs were determined by TEM. For this characterization 1 mg of silver NPs were dissolved in 1 mL (50%) ethanol and then sonicate it for 25 min to mix properly. A drop of 10 μl of each samples was dropped on para-film and put grid on it for 5–10 min. The next day the samples were observed under TEM (200Kv FEI Tecnai).

Fourier transform infrared (FTIR) spectroscopy (SHIMADZU 8100 M FTIR, Shimadzu, Kyoto, Japan) was performed (in the range of 500–4000 cm^{-1}) to study the bio-molecules presence as capping agents on silver NPs surface.

Table 1
Silymarin detection by HPLC form NP1, NP2, NP3 and NP4. (nd: not detected). Columns with similar alphabets (letters a–e) are not significantly different ($p \leq 0.05$).

Phytochemicals	NP1 µg/mg DW	NP2 µg/mg DW	NP3 µg/mg DW	NP4 µg/mg DW
Taxifolin	12.76 ± 1.12^{de}	229.11 ± 1.34^{de}	32.81 ± 1.59^{de}	371.26 ± 1.91^{d}
Silychristin	156.48 ± 1.45^{de}	458.84 ± 1.81^{d}	190.75 ± 1.23^{de}	543.41 ± 1.29^{cd}
Isosilychristin	131.91 ± 1.63^{de}	215.98 ± 1.67^{de}	154.21 ± 1.45^{de}	252.66 ± 1.32^{d}
Silydianin	527.40 ± 1.78^{cd}	784.41 ± 1.45^{c}	598.79 ± 1.67^{cd}	976.19 ± 1.28^{c}
Silybin A	6.41 ± 0.57^{e}	784.41 ± 1.34^{c}	598.79 ± 1.78^{cd}	976.19 ± 1.37^{c}
Silybin B	4.80 ± 0.07^{e}	1549.32 ± 1.27^{b}	10.98 ± 1.21^{e}	2289.22 ± 1.46^{a}
Isosilybin A	0.80 ± 0.03^{e}	558.05 ± 1.61^{cd}	3.92 ± 1.11^{e}	644.25 ± 1.59^{cd}
Isosilybin B	nd	427.51 ± 1.59^{d}	0.78 ± 0.02^{e}	486.46 ± 1.94^{d}
Total silymarin	0.84 ± 0.04^{e}	5.64 ± 1.47^{e}	1.00 ± 0.07^{e}	7.60 ± 1.11^{e}

3.2. Solid phase extraction procedure

For quantification and separation of compounds from NPs, solid phase cartridges (Sep Pak Plus C18 cartridges) were used (Table 1). In the extraction procedure the Visiprep SPE vacuum manifold (12-port model) from Supelco (Supelco, Saint-Quentin Fallavier, France) was used. The previously established protocol was followed for extraction [36].

3.3. HPLC analysis

In HPLC vials the samples were loaded and then quantified using Varian high performance liquid chromatography system equipped with Meta chem Degaist degasser, Varian Prostar 230 pump, Varian Prostar 335 Photodiode Array Detector (PAD) and Varian Prostar 410 autosampler, driven by Galaxie version 1.9.3.2 software (Varian, Le Plessis-Robinson, France). The isolated compounds standards for HPLC i.e. taxifolin, silychristin, isosilychristin, silydianin, silybin A, silybin B, isosilybin A, isosilybin B were obtained from Sigma Aldrich. The separation technique used was adapted from [37,38]. A particle size of 5 µm was prepared by guard column Alltech, 10 × 4.1 mm, Hypersil PEP 300 C18, 250 × 4.6 mm was used for separation at 35 °C. At a wavelength of 320 nm and 520 nm the compounds were detected. The mobile phase has two HPLC grade solvents i.e. A = $HCOOH/H_2O$, pH = 2.1, B = CH_3OH. The mobile phase composition vary throughout 1 h per run, with nonlinear gradient 8% B (36 min), 100% B (30–35 min), 33% B (28 min), 30% B (17 min), 12% B (11 min), and 8% B (0 min) at flow rate of 1 mL/min. A 10 min re-equilibration time among individual run was used. HPLC analysis shows that overall high content of silymarin was observed in NP4 followed by NP2, NP3 and NP1 respectively. Quantification was done to rely on reliable reference standards and an assessment of retention time. The samples were run thrice. The results were recorded as µg/mg DW of samples.

3.4. Biological assays

3.4.1. Antidiabetic and antioxidant activities

Briefly, dry powder of each sample (0.1 g) was homogenized with methanol (0.5 mL), and the mixture was sonicated (30 min) using the sonicator (VWR International, Fontenay-sous-Bois, France; inner dimension: 300 mm × 240 mm × 200 mm) and vortexed (5 min). The process was repeated thrice to well homogenize the samples. The samples were centrifuged at 12,000 rpm for 15 min, and the supernatant was separated and for further analysis stored at 4 °C.

3.4.2. α-Glucosidase inhibition

To purify and immobilize α-glucosidase the Rat intestinal acetone powder (Sigma, Saint Quentin Falavier, France) and CNBr-activated sepharose 4B (Sigma, Saint Quentin Falavier, France) were used respectively according to previous protocol [39]. By employing chromogenic method for the determination of immobilized enzymatic activity, the polyethylene filter (0.45 µm) with end-capped column was used as described previously. 1 µl intestinal fluid containing 4-nitrophenyl-α-D-glucopyranoside (5 mM, 4NPG; Sigma, Saint Quentin Falavier, France) was used to perform this assay. After 30 min incubation time 1 M sodium carbonate was added and the reaction stopped by column filtration. To determine the enzymatic activity against blank solution the absorbance was taken at 405 nm. The difference in values of absorbance in the presence and absence of samples was expressed as % inhibition.

3.4.3. α-Amylase inhibition

The α-amylase activity of test samples was determined by using well established protocol described previously [40] and the α-amylase from porcine pancreas was obtained from Sigma Aldrich. Briefly, to prepare enzyme at 1 µ/mL concentration the phosphate buffer (0.1 M; pH 6.8) was used and 4-nitrophenyl-α-D-maltopentaoside (5 mM, 4NPM; Sigma) was continuously mixed with it. The reaction mixture was provided an incubation time of 30 min in the presence and absence of samples at room temperature. The reaction stopped with 1 M sodium carbonate solution and at 405 nm the absorbance was taken using Synergy II reader (BioTek Instruments, Colmar, France) for determination of enzymatic activity against blank solution. The difference in values of absorbance in the presence and absence of samples was expressed as % inhibition.

3.4.4. ABTS antioxidant assay

For ABTS (2,2-azinobis-3-ethylbenzthiazoline-6-sulphonic acid) assay the method described by Velioglu et al. [48] was employed. For preparation of ABTS solution, 7 mM ABTS salt was mixed with equal proportion of potassium per sulphate 2.45 mM and the mixture was then kept for 16 h in dark. The absorbance of solution was recorded at 734 nm and, it was adjusted to 0.7 prior to mixing with extracts and extracts mediated AgNPs. Again the mixture was put at room temperature (25 ± 1 °C) for 15 min in dark and at 734 nm the absorbance was recorded with the help of microplate reader (Bio Tek ELX800 Absorbance Microplate Reader, BioTek Instruments, Colmar, France). The antioxidant activity was expressed in TEAC and performed in triplicates.

3.4.5. FRAP (ferric reducing antioxidant power) assay

Strain and Benzie method [42] was followed to perform this assay. Briefly, FRAP solution 190 µL [containing 2,4,6-Tri (2-pyridyl)-s-triazine (TPTZ; 10 mM); ferric chloride hexahydrate ($FeCL_3.6H_2O$) 20 mM, acetate buffer (300 mM) of pH 3.6; ratio 10:1:1 (v/v/v) was mixed 10 µL samples. The reaction mixture was put at room temperature for 15 min. The absorbance was recorded at 630 nm using microplate reader (BioTek ELX800 Absorbance Microplate Reader, BioTek Instruments, Colmar, France). The activity was demonstrated as TEAC and the activity was performed in triplicates.

3.4.6. DPPH activity

The free radical scavenging activity, DPPH (2,2-diphenyl-1-picrylhydrazyl) of each sample using Abbasi et al. protocol [43] was performed. To each well of the microplate the sample (20 μL) was added, followed by addition of 180 μL DPPH reagent solution and then kept for 60 min at room temperature in the dark. Final concentrations of Ascorbic acid (05, 10, 20 and 40 μg/mL) and DMSO (20 μL) with DPPH (180 μL) were taken as negative control. At 517 nm the absorbance of solution was recorded using microplate reader (BioTek ELX800 Absorbance Microplate Reader, BioTek Instruments, Colmar, France). To calculate activity of DPPH, the following formula was used:

$$\%\text{scavenging} = 100 \times (1 - \text{AE/AD}) \quad (1)$$

where AD = DPPH solution absorbance without addition of any material, and AE = the absorbance of mixture with sample addition at 517 nm.

3.4.7. Total antioxidant capacity (TAC)

The phosphomolybdenum based assay was used to carry out samples assessment of total antioxidant capacity [44]. DMSO amounting 100 μL (negative control) and test sample amounting 4 mg/mL (dissolved in DMSO) were added separately to reagent (900 μL) containing sodium phosphate, ammonium molybdate and sulphuric acid having 28 mM, 4 mM, and 0.6 mM concentrations respectively. To complete the reaction the mixture was incubated at 95 °C for 90 min in water bath. The absorbance of test solutions and standard after cooling was recorded at 695 nm by spectrophotometer (8354 Agilent Technologies, Waldbronn, Germany). DMSO was used as blank reading. The experiment was done in triplicate. The antioxidant activity measured corresponds to ascorbic acid dry weight (μg/mg) equal to antioxidant capacity (μg AAE/mg DW).

3.4.8. Total reducing power (TRP)

Potassium ferricyanide assay was used to calculate the reducing power of test samples [45]. Ferricyanide amounting 400 μL (1%) was taken in phosphate buffer 0.2 mol/L (pH 6.6) to which test sample (4 mg/mL dissolved in DMSO) amounting 100 μL was added. The mixture was then incubated for 20 min at 50 °C. After incubation trichloroacetic acid (10%) amounting 400 μL was added to all the test samples. The mixture was then centrifuged at 3000 rpm for 10 min at room temperature. Supernatant amounting 500 μL was collected to which 0.1% $FeCl_3$ amounting 100 μL and distilled water 500 μL was added. The optical density was recorded at 700 nm using microplate reader (Platos R, 496. AMP, AMEDA Labordiagnostik GmbH, Graz, Austria). Ascorbic acid and DMSO were taken as positive and negative control respectively. Reducing power of samples corresponds to dry weight of ascorbic acid (μg/mg) equivalent antioxidant ability (μg AAE/mg DW).

3.5. Anti-aging

3.5.1. Collagenase assay

For this assay the collagenase clostridium histolyticum (Sigma Aldrich) was used and the activity was determined with the help of spectrophotometer by using substrate *N*-[3-(2-furyl)acryloyl]-Leu-Gly-Pro-Ala (FALGPA; Sigma Aldrich) according to Wittenauer et al. (2015) [46]. The FALGPA absorbance decrease was followed for 20 min at 335 nm using microplate reader (BioTek ELX800; BioTek Instruments, Colmar, France). The measurements were used in triplicates and the activity was shown as % inhibition relative to control (adding same volume of extraction solvent) for each extract.

3.5.2. Elastase assay

Porcine pancreatic elastase (Sigma Aldrich) was used to perform Elastase assay by using substrate *N*-Succ-Ala-Ala-Ala-*p*-nitroanilide (AAAVPN; Sigma Aldrich) and spectrophotometer for activity determination and following release of p-nitroaniline at 410 nm using microplate reader (BioTek ELX800; BioTek Instruments) following Wittenauer et al. (2015) method [46]. The measurements were made in triplicates and anti-elastase activity was shown in % inhibition relative to control (adding same volume of extraction solvent) for each extract.

3.5.3. Hyaluronidase assay

Using the protocol of Kolakul et al. (2017) the Hyaluronidase assay was performed using hyaluronic acid solution (0.03% (*w/v*) and 1.5 hyaluronidase units (Sigma Aldrich) as substrate [47]. With acid albumin solution (0.03% (w/v) BSA, the precipitation of hyaluronic acid (undigested form) occurred. At 600 nm the absorbance was measured using microplate reader (BioTek ELX800; BioTek Instruments, Colmar, France). The measurements were made in triplicates and hyaluronidase inhibitory effect was shown in % inhibition relative to control (adding same volume of extraction solvent) for each extract.

3.5.4. Tyrosinase assay

To determine tyrosinase assay Chai et al. (2018) method was used [48]. Briefly, L-DOPA (5 mM; Sigma Aldrich) was utilized as diphenolase substrate and then mixed in sodium phosphate buffer (50 mM, pH 6.8) with 10 μL of each sample. To make a final volume of 200 μL, a solution mushroom tyrosine (0.2 mg/mL; Sigma Aldrich) was added. For replacing the extract an equal amount of solvent extraction (Control) was regularly carried out. At 475 nm the absorbance of the reaction was traced using microplate reader (BioTek ELX800; BioTek Instruments). The measurements were made in triplicates and tyrosinase inhibitory effect was shown in % inhibition relative to control (adding same volume of extraction solvent) for each extract.

3.5.5. Vesperlysine and pentosidine-like AGEs activity

Following the protocol of Siriamornpun and Kaewseejan (2015) [49] the inhibitory ability of AGE formation was measured. Each sample was mixed with 20 mg/mL BSA solution (Sigma Aldrich) prepared in phosphate buffer (0.1 M; pH 7.4), glucose solution (0.5 M; Sigma Aldrich) prepared in phosphate buffer and 1 mL phosphate buffer (0.1 M; pH 7.4) containing sodium azide 0.02% (*w/v*). the mixture was incubated for five days at 37 °C in dark and the fluorescent AGE amount formed was measured using fluorescence (VersaFluor fluorometr; Bio-Rad, Marnes-la-Coquette, France) set with 410 nm emission and 330 nm excitation wavelength respectively. The anti-AGEs percentage formation was shown in % inhibition relative to control (adding same volume of extraction solvent) for each extract.

3.5.6. SIRT-1 assay

Using SIRT1 Assay Kit (Sigma Aldrich), the activity was determined following the instructions of manufacturer and fluorescent spectrometer (Biorad VersaFlour, Marnes-la-Coquette, France) set at 430 nm emission and 340 nm excitation wavelength respectively. The SIRT1 activity was shown in % relative to control (adding same volume of extraction solvent) for each extract.

3.6. Anti-inflammatory activities

3.6.1. COX-1 and COX-2

To check the inhibitory activities of the samples against COX-1 and COX-2 using COX-1 (Ovine) and COX-2 (human) assay kit (701,050, Cayman Chem. Co, Interchim, Montluçon, France) was used following the manufacturer instructions. The positive control was taken ibuprofen (10 μM) and arachidonic acid (1.1 mM concentration) as a substrate. Using kit the components of COXs peroxidase were measured. At 590 nm the Synergy II reader (BioTek Instruments, Colmar, France) for 5 min in 96-well microplate was used to check oxidized *N*,*N*,*N*′,*N*′-tetramethyl-*p*-phenylenediamine.

3.6.2. Inhibitory activity against 15-LOX

The assay kit (760700, Cayman Chem. Co., Interchim, Montlçuon, France) was used according to manufacturer instructions to check inhibitory activity of test samples against 15-LOX. The positive control inhibitor was taken as nordihydroguaiaretic acid (NDGA; 100 μM) while arachidonic acid (10 μM) was taken as substrate. During lipooxygenation reaction the hydroperoxides concentration produced was measured by kit using filtered soy 15-lipooxygenase standard in Tris-HCl buffer (10 mM) at pH 7.4. For measurement in 96-well microplate the Synergy II reader (BioTek Instruments, Colmar, France) was used at 940 nm. After incubation of enzyme and inhibitor for 5 min, the absorbance was noticed followed by substrate addition and 15 min incubation and then followed by chromogen addition and 5 min incubation.

3.6.3. Inhibitory activity against secretory phospholipase A2 (sPLA2)

An essay kit (10004883, Cayman Chem. Co, Interchim, Montlçuon, France) was used according to the manufacturer instructions for the inhibitory ability of the test samples against sPLA2. The positive control inhibitor was taken thiotheramide-PC (100 μM) while diheptanoyl-PC (1.44 mM) was taken as substrate. Free thiols were released by the breakdown of diheptanoyl thio-PC ester which is measured in 96-well microplate at 420 nm using Synergy II reader (BioTek Instruments, Colmar, France) using DTNB (5–5′-dithio-bis-(2-nitrobenzoic acid). The percent inhibition was calculated using formula:

$$\%\text{Inhibition} = [(\text{IA}-\text{Inhibitor})/\text{IA}] \times 100 \quad (2)$$

3.7. Statistical analysis

The experiments were performed in triplicate and for statistical analysis XL-stat_2018 (Addinsoft, Paris, France) was used.

3.8. Cytotoxicity screening

3.8.1. Cell culture

In DMEM the hepatocellular carcinoma cells (ATCC HB-8065) were cultured which contain 2 mM L-glutamine, Fetal calf serum 10% (FCS), 100 U/mL penicillin, 1 mM Na-puruvate, and streptomycin (100 μg/mL) in a humidified 5% CO_2 atmosphere at 37 °C. The harvesting of cells was done at room temperature (25 ± 1) with 0.5 mM trypsin/EDTA for 1 min.

3.8.2. Sulforhodamine B (SRB) assay

For cytotoxicity screening the extracts were dissolved in DMSO and NPs were suspended in deionized water. In 96-well plate the HepG2 cells (> 90% confluency) were seeded at density of 12,000 cells/well and were the allowed to adhere at 37 °C at 24 h. Then the cells were treated for 24 h with NPs/Extracts (200 μg/mL). For fixing the cells pre-chilled 50% Trichloroacetic acid (TCA) were used and incubated for 1 h at 4 °C, followed by thrice rinsing with deionized water. The air dried plates having cells were then stained with SRB dye 0.01% followed by incubation at room temperature (25 ± 1) for 30 min and washing with acetic acid (1%) for unbound dye removal. DMSO 1% and Non-treated Cells (NTC) were taken as controls. The background optical density was represented by Blanks which consist of media and samples controls only. Equipped with digital camera the Olympus CK2 light microscope was used for photographs. Each sample was run in triplicates and the experiment was repeated twice. For solubilizing SRB dye 100 μL Tris (10 mM; pH 8) was added to each well for 5 min at room temperature. Using Microplate reader (Platos R 496, AMP) the absorbance values were measured at wavelength of 565 nm. For calculating the percentage viability relative to untreated samples the following formula was used:

$$\text{Viability}\ (\%) = \frac{\text{Abs}\ (565)_{\text{sample}} - \text{Abs}\ (565)_{\text{Extract/NPcontrol}}}{\text{Abs}\ (565)_{\text{NTC}} - \text{Abs}\ (565)_{\text{Blank}}} \times 100 \text{whereas} \quad \text{Abs}$$

(565) $_{\text{NTC}}$ and Abs (565) $_{\text{sample}}$ represent optical density of NTC and treated samples respectively. Abs (565) $_{\text{Blank}}$ and Abs (565) $_{\text{NTC}}$ are representative of background measured OD for media and extracts/NPs samples only.

3.9. Antibacterial and antifungal activities

The antibacterial and antifungal efficacies of NP3, NP1, NP4 and NP2 were evaluated against four different multi-drug resistant (MDR) pathogenic bacteria (*Klebsiella pneumonia ATCC 70063*, *Staphylococcus aureus ATCC 43300*, *Escherichia coli 25922*, *Enterobacter intermedius NCTC 12125* and one pathogenic strain of fungi (*Candida albicans ATCC 10231*), by performing well diffusion method. 15 mg of each NP3, NP1, NP4 and NP2 were dissolved separately in 1 mL of sterile deionized water. 15 mg/mL Ciprofloxacin powder and 10 mg/mL Amphotericin B were used as positive control for Bacteria and Fungi respectively. $AgNO_3$ salt 0.02 M was used as negative control. Overnight growth suspension of 0.5 MacFarland turbidity standard was used for bacterial and fungal lawn formation. Petri plates containing media were swabbed with bacterial and fungal strains, wells were loaded with desired extracts and were kept at 37 °C in incubator. After 24 h incubation, zone of inhibition was measured in millimetre by Vernier caliper. The activity was repeated three times and values were recorded.

4. Results and discussion

4.1. UV-spectroscopy

The addition of silver nitrate solution (1 mM) to the seed extract (1:5) respectively resulted in change in color from transparent to yellowish brown, which is an indication of AgNPs synthesis. Not much change in color was observed after 24 h and aggregates were observed settling down after 24 h and hence, at this time period, the absorbance was recorded using UV–vis spectroscopy. The surface Plasmon resonance (SPR) of AgNPs produced peak near 448 nm (Fig. 1). The absorbance peak was recorded near 448 nm indicating $AgNO_3$ reduction into AgNPs. Similarly, $AgNO_3$ was added to the wild *Silybum* extract (1:2) respectively and color changes were noticed which shows the synthesis of AgNPs. The absorbance peak was recorded at 430 nm indicating $AgNO_3$ reduction into silver NPs. The change in color of the solution is due to excitation of surface Plasmon vibrations with AgNPs. Our results are similar to the previous reports [50]. The solution mixtures were kept for 72 h to monitor the complete reduction of Ag ions into AgNPs. No change in color or absorbance was observed after 72 h, which indicate the complete reduction of all Ag ions into AgNPs.

4.2. FTIR

Several phytochemicals are involved in the capping and stabilization of biosynthesized NPs. FTIR is a powerful tool to analyze the functional groups that are involved in capping NPs. The FTIR spectra of NP3 showed various peaks at 3287.7 cm^{-1}, 2922.8 cm^{-1}, 2852.9 cm^{-1}, 1742.6 cm^{-1}, 1653.1 cm^{-1}, 1537.3 cm^{-1}, 1456.1 cm^{-1}, 1045.0 cm^{-1} and 518.3 cm^{-1} whereas the peaks for NP1 were observed at 3286.1 cm^{-1}, 2922.7 cm^{-1}, 1561.1 cm^{-1}, 1387.3 cm^{-1}, 1036.7 cm^{-1}, 666.5 cm^{-1} and 521.1 cm^{-1} (Fig. 2). The broad peaks obtained in the range of 3287.7 cm^{-1} and 3286.1 cm^{-1} represents O—H stretching vibrations of alcoholic phytochemicals. Peaks observed at 2922.8 cm^{-1} and 2922.7 cm^{-1} represents stretching in C—H bonds of aromatic compounds [51]. The peaks ranging between 1742.6 cm^{-1} and 1653.1 cm^{-1} represents C═O linkages in aldehydes whereas the peak at 1456.1 cm^{-1} shows C—H stretching in alkenes [52]. Peaks may be attributed to N—O asymmetric stretching vibrations [53]. The peak at 1387.3 cm^{-1} is due to -C-O-like phenol groups [54] while peaks at 1045.0 cm^{-1} and 1036.7 cm^{-1} represents C—O stretching vibrations [55]. Our results are in similarity with the previous report [56].

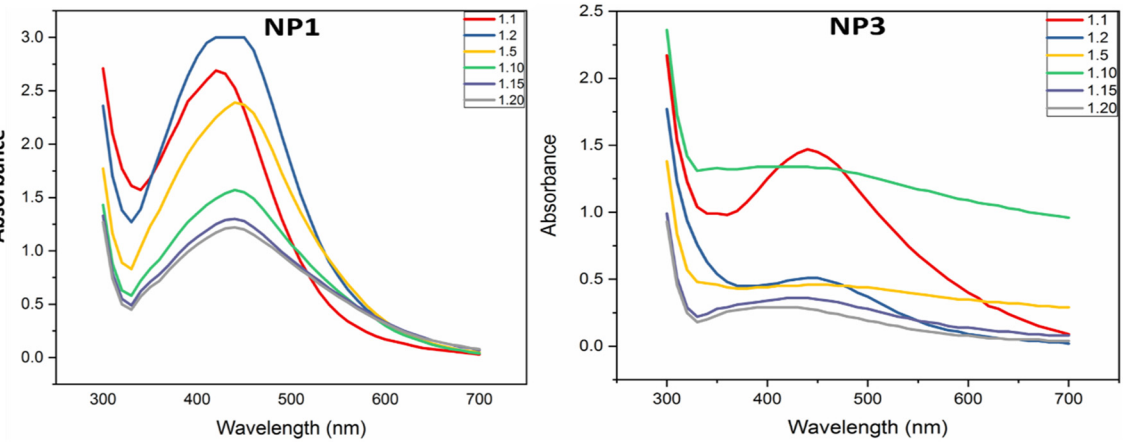

Fig. 1. UV-spectroscopy of NP1 and NP3

4.3. X-ray diffraction analysis

XRD analysis was carried out for Seed and Wild mediated Ag-NPs to confirm its crystalline nature. The seed mediated Ag-NPs suggested crystalline nature as the peaks were observed according to JCPDS File no. 04-0784. The peaks at the range of 20–70° correspond to (98), (101), (111), (200) and (220) as shown in Fig. 3(A). Comparison to others wild mediated Ag-NPs carries three intense peaks which gives surety to crystalline nature. The peaks were confirmed by JCPDS File no. 04–0784, which corresponds to (111), (200) and (220) as shown in Fig. 3 (B). Using Scherrer equation the size of NP1 and NP3 was 18.12 nm and 13.20 nm respectively. Our results are in harmony with previous studies [57,58].

4.4. Transmission electron microscopy

The surface morphology and size distribution of green synthesized AgNPs were confirmed through TEM analysis. Granular like morphology was observed for both NP1 and NP3. In case of both NP1 and NP3, small rounded or spherical shaped morphology with regular shapes were noticed. The particles are highly monodispersed. Our results are similar to previous studies [59,60]. Considering TEM precision, we consider that the sizes of these AgNPs are in close proximity to the calculated size following XRD analysis using Debye Scherrer equation. The average size of NP1 is approximately 22 nm while the average size of NP3 is 19 nm (Fig. 4).

4.5. Zeta size and zeta potential analysis

The dynamic size and surface potential of the as-synthesized NPs were acquired with DLS. Before analysis, the samples were highly dispersed in water with ultrasonication with the objective to maintain the polydispersity index (PDI) below than 0.5 that is highly needed during analysis. As shown in the Fig. 5, three peaks in NP1 and two peaks in the NP3 with low and high intensity were observed. However, the peaks with high intensity around 140 nm in both samples validate the uniformly distributed NPs as observed in TEM analysis. Similarly, the small peaks around 10 nm and 20 nm also indicate the size of NPs, However, based on the peak with high intensity display the large size of NPs esteemed from DLS, that is not unusual. It is generally believed, that size

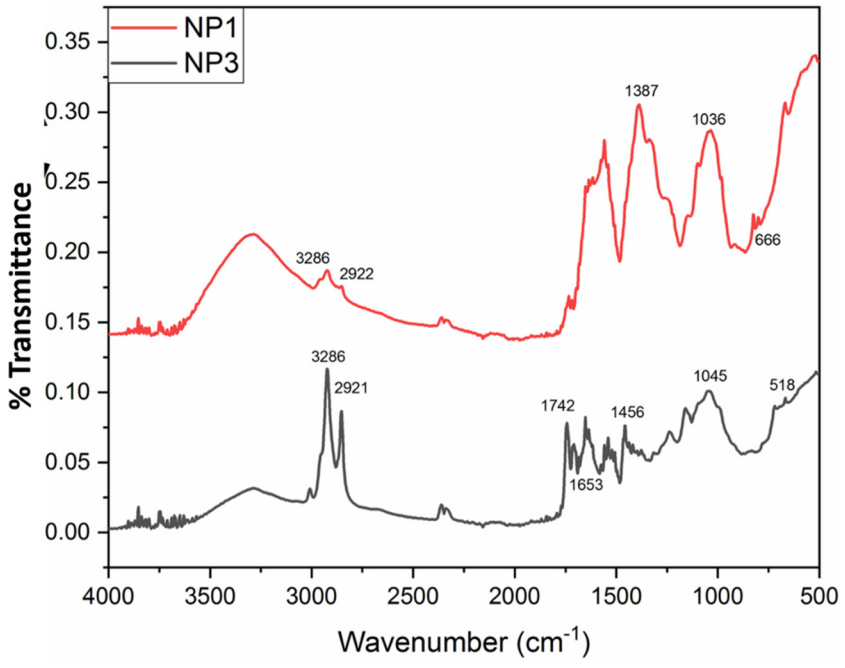

Fig. 2. FTIR analysis of NP1 and NP3 respectively.

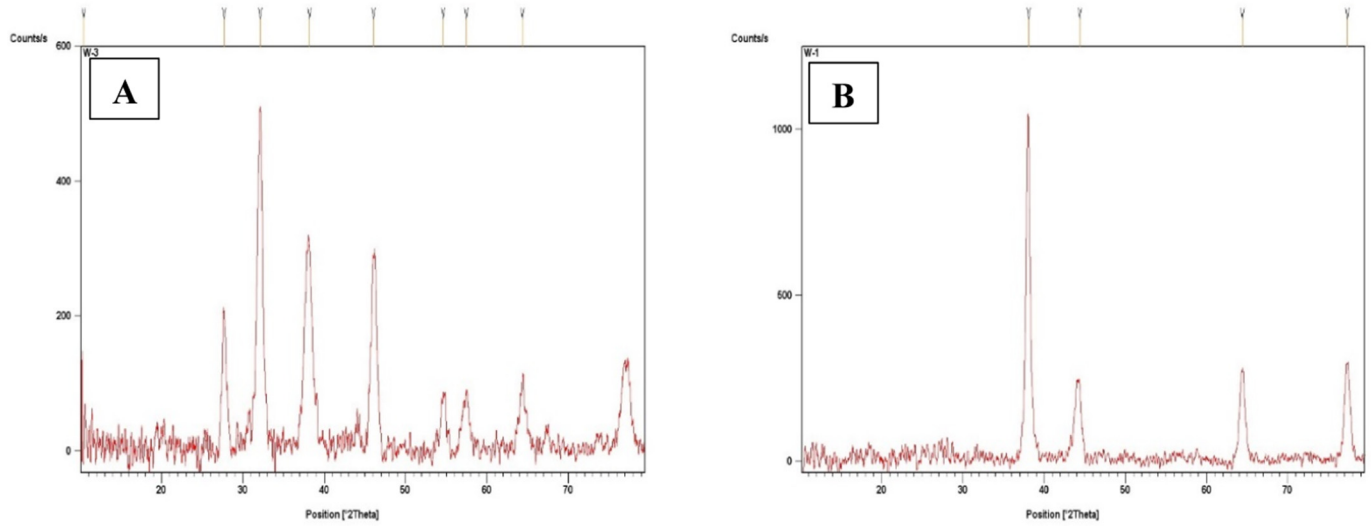

Fig. 3. XRD analysis of NP1 (A) and NP3 (B).

determined based on DLS is usually higher than the respective size calculated from SEM/TEM, because DLS measure the hydrodynamic size (size and surface water molecule). In addition, the agglomeration or poor dispersion significantly increase the average value and thus generally contradict the SEM/TEM results. Further, the surface potential was also determined under the same conditions. As shown in the Fig. 5, expectedly, the sharp peaks at the negative potential of −10 mV and −17 mV were observed for NP1 and NP3 respectively. The negative potential on the surface of metal oxide NPs is usual especially when using the plant extract. During the calcination process, the functionality like OH and OOH retain the on the surface of NPs which warrant the negative zeta potential to the overall material. In addition, the negative potential with single peaks not only suggests the uniform distribution of surface charge but also validate the stability of the material in aqueous medium.

4.6. HPLC and SPE analysis

Solid phase extraction is used for component separation, isolation and/or adsorption from liquid phase (sample) to stationary phase (sorbent or resin). It is same like digital chromatography. For the past 20 years SPE is considered as the most dynamic method for rapid and selective preparation of sample before analytical chromatography. For numerous samples the most extensive technique SPE is used [61]. There are many advantages of SPE technique like high enhancement factor, easy operation, effective matrix interference, fast separation phase, minimum solvents consumption, cost effective and maximum recovery [62].

Recently the nanoscale metal oxides are more attractive to researchers compare to conventional adsorbents, given their rapid absorption kinetics and high surface area. Less reports have confirmed that NPs were high adsorbent materials and used in SPE extraction procedure [63].

HPLC includes quantification of silymarin compounds from NP1

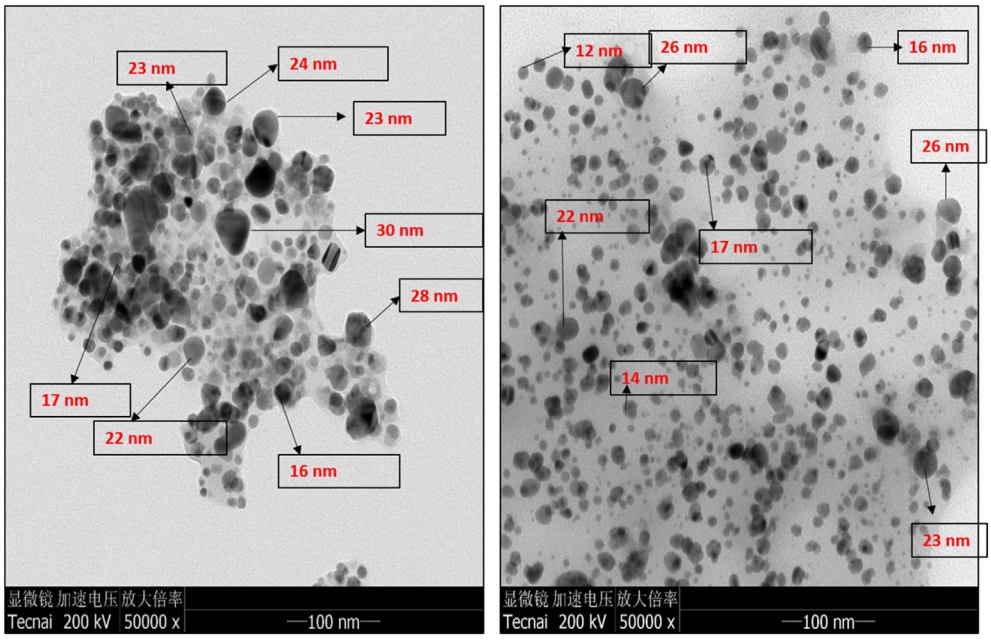

Fig. 4. Displays TEM images of NP1 (A) and NP3 (B).

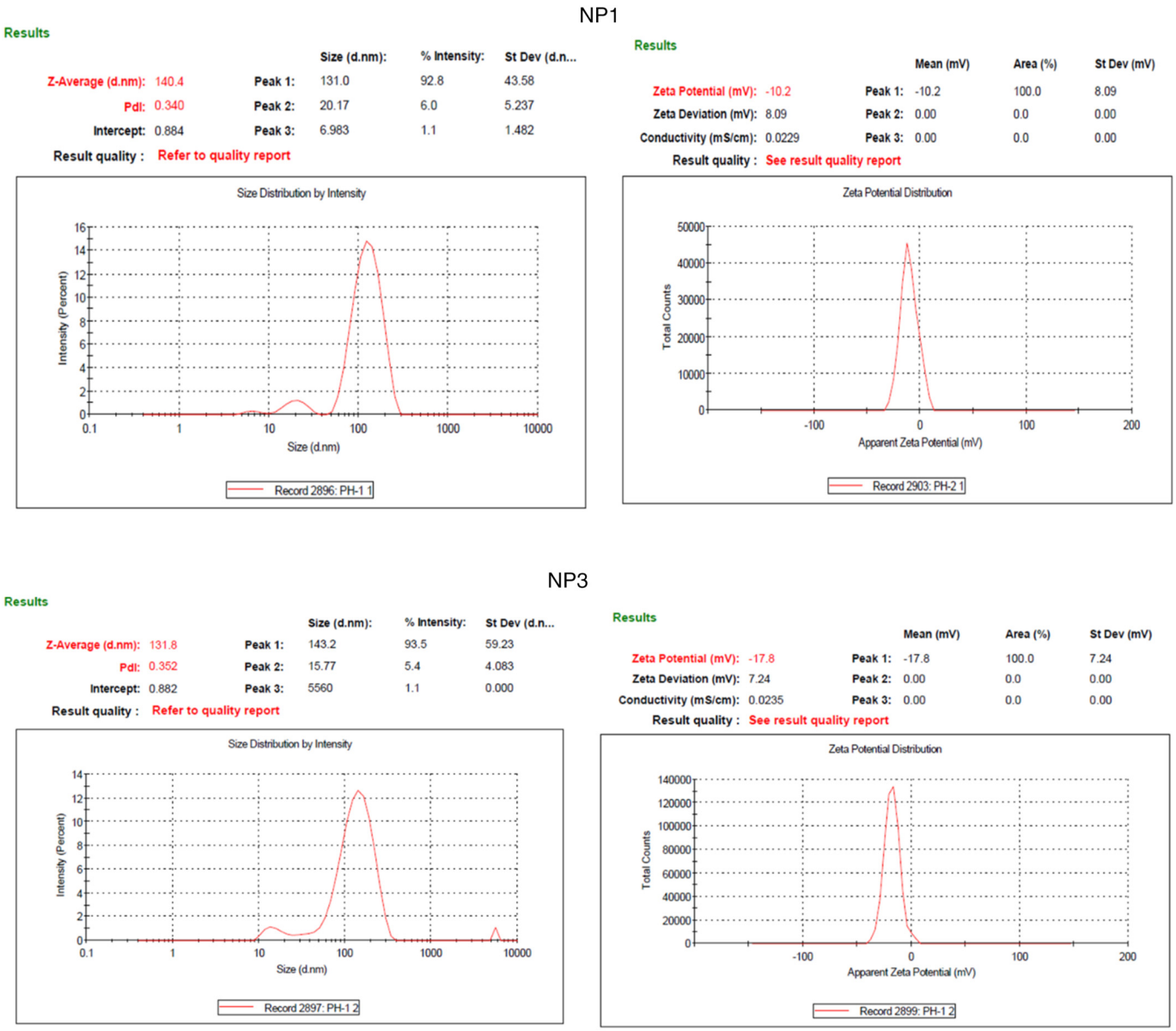

Fig. 5. Shows zeta size and potential of NP1 (A) and NP3 (B) respectively.

(Wild *Silybum* NPs), NP2 (Wild extract), NP3 (Seed NPs), NP4 (Seed extract) previously described by Drouet et al. [64] and compared with commercial AgNPs. It was observed that NP1, NP2, NP3 and NP4 showed silymarin in a specific amount (silychristin, isosilychristin, silydianin, silybin A, silybin B, isosilybin A, isosilybin B, and taxifolin) which indicates that these secondary metabolites might be responsible capping agents. Due to high number of "OH" group and increased value of Silydianin in both NP1 and NP3, it is believed as the best capping agent. The flavonoids and phenols act as reducing and stabilizing agents for NPs synthesis, these components are responsible for reducing Ag ions to AgNPs [65]. Silychristin, silydianin and to a less extend isosilychristin are the main "capping" phytochemicals for both NPs samples (NP1 and NP3). Only isosilybin B is below the LOQ for NP1 (but trace of this compound is detected). For plant materials NP4 is richer as compared to NP2 sample. NP4 ("seed", i.e. fruit) contents are in the range of our previously described contents for *Silybum* ecotypes from Pakistan [66]. The results indicate that active reducing agent in NP1, NP2, NP3 and NP4 was silymarin, which results in metal ions reduction into metal NPs. There are several reports available in literature on silymarin as stabilizing and reducing agent in callus extract [67,68].

5. Biological activities

5.1. Antioxidant

The shift in the metabolic pathways of plants is due to environmental stress which produces reactive oxygen species (ROS) that damage membrane lipids, plant cells, DNA and proteins [69]. Plants produce various metabolic compounds like flavonoids, terpenoids and phenolics to oxidative stress response which act as mechanism of protection [70,71]. In this paper the antioxidant potential of *Silybum* (Seeds, wild plant) based NPs and their extracts were explored by using three antioxidant assay i.e., DPPH (2,2-diphenyl-1-picrylhydrazyl) assay (mixt Hydrogen atom transfer (HAT)- and electron transfer (ET)-based antioxidant assay), FRAP (ferric reducing activity) assay (ET-based antioxidant activity) and ABTS (2,2-azinobis-3-ethylbenzthiazoline-6-sulphonic acid) assay. Due to the mixed ET- and HAT-based antioxidant mechanism, DPPH free radical reducing activity was shown as % of free radical scavenging activity, whereas the FRAP and ABTS activities were indicated as TEAC (trolox C equivalent antioxidant capacity, μM). Highest DPPH (83.5 ± 1.6% μgAAE/mg) was shown by NP4

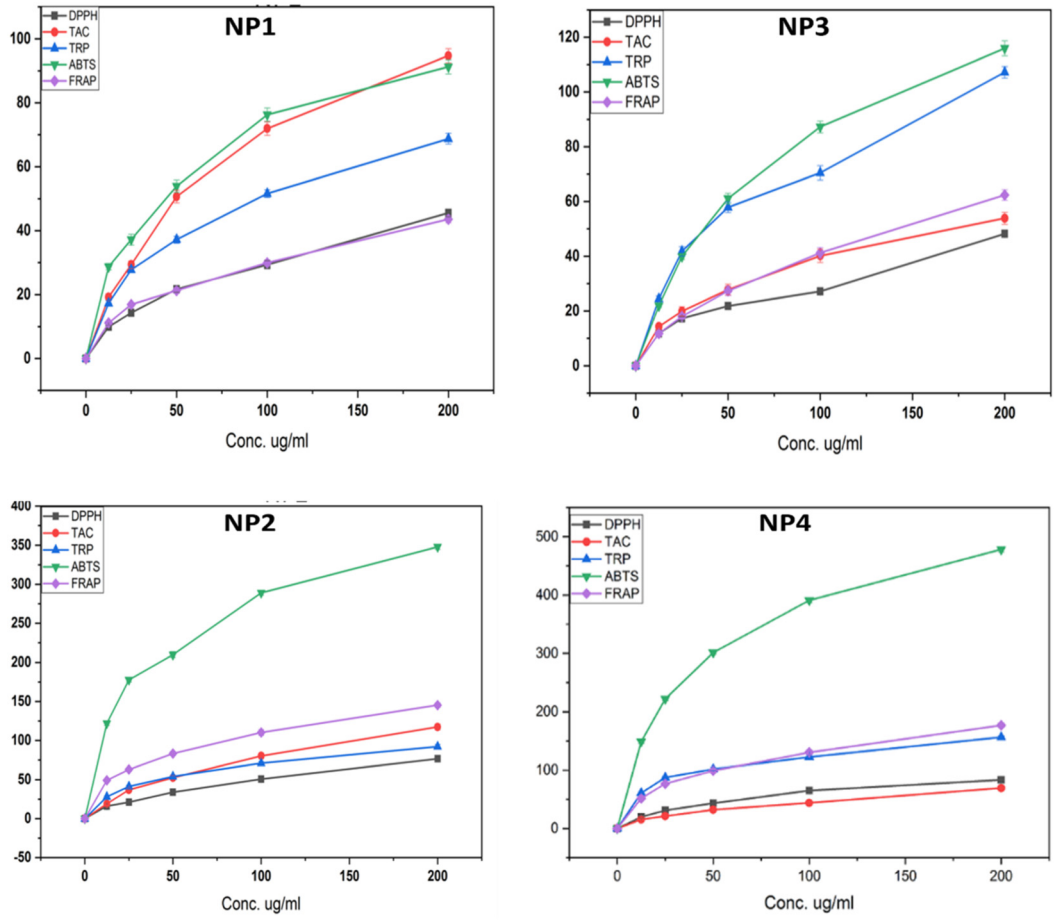

Fig. 6. DPPH, TAC, TRP, ABTS and FRAP of NP1, NP3, NP2 and NP4 respectively.

Table 2
Anti-inflammatory activity of test samples. Columns with similar alphabets (letters a–b) are not significantly different ($p \leq 0.05$).

Sample names	NP1	NP2	NP3	NP4
COX-1	12.45 ± 1.34^{b}	38.56 ± 1.29^{a}	14.56 ± 0.87^{b}	34.52 ± 1.37^{a}
COX-2	11.87 ± 1.94^{b}	27.65 ± 1.73^{ab}	12.52 ± 2.01^{b}	24.26 ± 0.73^{ab}
15-LOX	16.12 ± 1.67^{b}	32.45 ± 1.64^{a}	17.85 ± 1.62^{ab}	38.41 ± 1.57^{a}
sPLA2	9.54 ± 0.95^{b}	25.64 ± 1.54^{ab}	10.54 ± 1.83^{b}	30.47 ± 0.91^{a}

Table 3
Anti-aging activities of four *Silybum* samples (2 extracts and 2 NPs) shown as % activities of control (DMSO). Columns with similar alphabets (letters a-c) are not significantly different ($p \leq 0.05$).

Sample name	NP1	NP2	NP3	NP4
Vesperlysine-like AGEs	28.74 ± 1.17^{ab}	41.95 ± 1.09^{a}	32.15 ± ^{ab}	44.46 ± 1.12^{a}
Pentosidine-like AGEs	29.52 ± 1.78^{ab}	47.64 ± 1.67^{a}	33.15 ± ^{ab}	48.89 ± 1.34^{a}
Tyrosinase	8.63 ± 0.81^{bc}	20.42 ± 1.65^{b}	10.45 ± 1.01^{bc}	24.63 ± 1.58^{b}
Elastase	5.23 ± 0.73^{c}	11.54 ± 1.34^{bc}	5.63 ± 0.75^{c}	14.52 ± 1.12^{bc}
Hyaluronidase	7.45 ± 0.78^{c}	8.15 ± 0.81^{bc}	6.96 ± 0.65^{c}	12.03 ± 1.09^{bc}
Collagenase	5.36 ± 0.75^{c}	22.46 ± 1.64^{b}	4.54 ± 0.72^{c}	23.68 ± 1.27^{b}

Table 4
Anti-diabetic potential of *Silybum* extract and NPs. Columns with similar alphabets (letters a–b) are not significantly different ($p \leq 0.05$).

Sample name	NP1	NP2	NP3	NP4
α-Glucosidase	22.45 ± 0.78^{b}	31.75 ± 1.67^{ab}	25.41 ± 1.37^{b}	32.62 ± 1.81^{ab}
α-Amylase	25.36 ± 1.12^{b}	38.41 ± 1.54^{a}	26.78 ± 1.43^{b}	38.74 ± 1.09^{a}

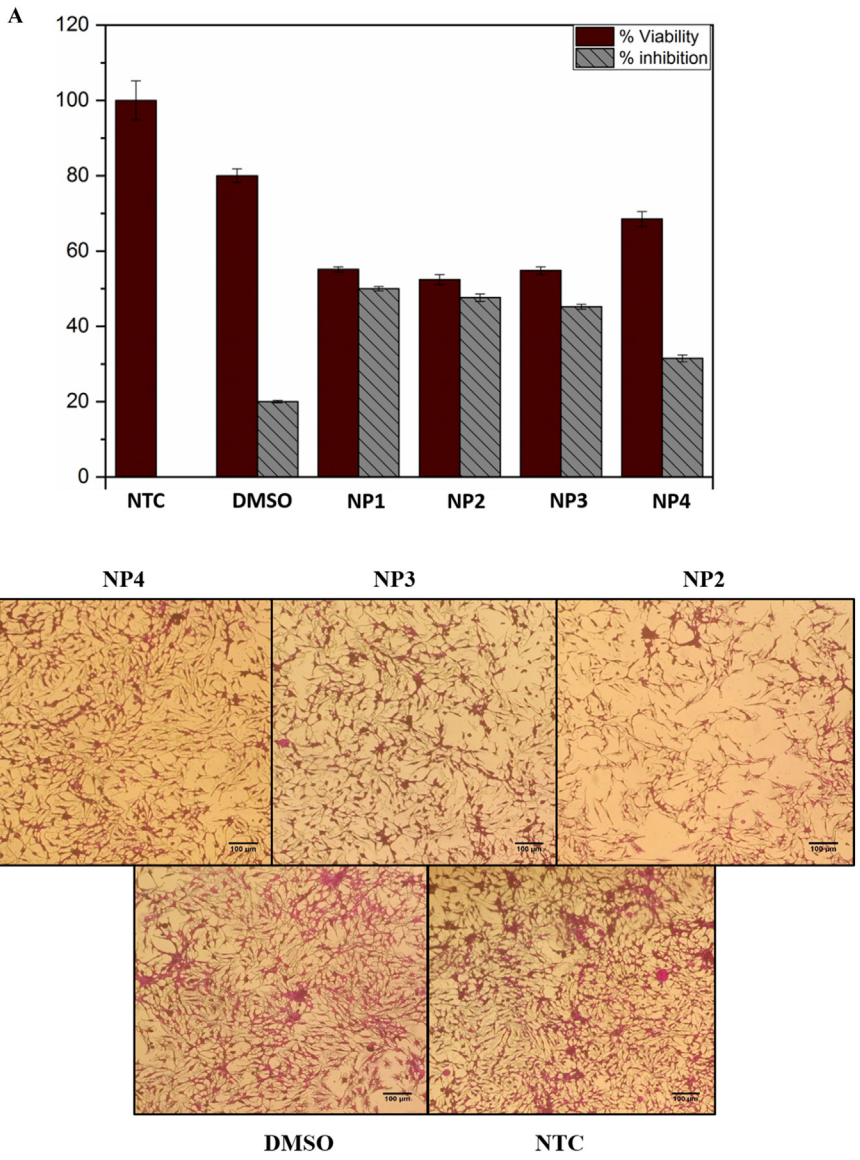

Fig. 7. A. Percentage viabilities (Mean ± SD) of treated HepG2 cells relative to untreated cells. Experiment was performed twice with replicates for each sample.
NTC = non-treated HepG2 cells; sample conc: stock provided 1% (200 µg/mL stock), SD = standard deviation. The experiments were performed in triplicates. NP1, NP2, and NP3 showed moderate inhibition with viabilities ranging from 52 to 55%. Whereas, NP4 showed slight cytotoxic effect (percent viability = 68.5%) respectively. The bars are mean ± standard deviation of the original data. The significant differences are indicated by different letters between conditions ($p < 0.05$).
B. Microscopic image of HepG2 cells (treated and untreated). Cells were treated with dose of NPs (NP1 and NP3) and extracts (NP2 and NP4) for 24 h. Untreated cells and DMSO were included as controls. Magnification = 100×, scale bar = 100 µm.

followed by NP2 (76.6 ± 1.3% µgAAE/mg). The TAC of NP2 was 117.35 ± 0.9 (µgAAE/mg) followed by NP4 69.3 ± 0.7 µg AAE/mg. Similarly the TRP was measured where the highest value of 156.3 ± 0.9 µg AAE/mg was shown by NP4 followed by the NP2 92.1 ± 1.3 µg AAE/mg. The ABTS value of NP4 is highest (478.23 µM) followed by NP2 (347 µM), NP3 (115.9 µM) and NP1 (91.2 µM), respectively (Fig. 6). Also the FRAP activity showed the same trend where the NP4 has the highest value of 176.91 µM, followed by NP2 145 µM, NP3 62.3 µM and NP1 43.58 µM, respectively. The results of antioxidant activities show a correlation with secondary metabolites of plants. Our results matches with previous reports [72,73].

5.2. Anti-inflammatory activities

Inflammation is the response of immune system to harmful stimuli, damaged cells, irritants and pathogens. The in vivo and in vitro anti-inflammatory activities for several flavonoids have been reported. Various mechanisms are exerted during in vivo anti-inflammatory action by these flavonoids like cyclooxygenase inhibition with a differential action on COX-2 vs. COX-1, Lipoxygenase (eicosanoid generating enzymes) and phospholipase A2, thereby decreasing prostanoid and leukotrienes concentrations [74]. To verify the anti-inflammatory activity of the test samples various in vitro assays like COX-2, COX-1, sPLA2 and 15-LOX were performed. The highest anti-inflammatory of all the samples was shown by NP2 (38.56 ± 1.29) against COX-1, followed by NP4 (38.41 ± 1.57, 34.52 ± 1.37) against 15-LOX and COX-1, respectively. The percent inhibition of other different samples is shown in the Table 2. The previous studies have shown that the enhanced anti-inflammatory activity is due to silymarin content in *S. marianum* [75,76]. The increased silymarin content production enhances the anti-inflammatory activity significantly was also concluded by Pradhan et al. [77]. The plants phytochemicals are solely responsible for the inhibition of enzymes that causes body inflammation [78,79].

5.3. Anti-aging activities

Anti-aging activity was determined to check the in vitro abilities of the test samples; (1) To inhibit hyaluronidase, elastase, AGEs and tyrosinase, collagenase (Matrix Metalloproteinase type 1 (MMP1)), and (2) to activate the activity of SIR-T1. The ability of degrading extracellular matrix components in dermis was found in collagenase, elastase and hyaluronidase, thus leading to alterations of skin including resilience losses, skin tonus and deep wrinkles [80,81]. Age-related diseases and aging are associated with oxidative stress [82] that leads to the building of AGEs (advanced glycation end products) [83]. The classical radical theory of aging has been challenged by several studies [84] and SIRT-1

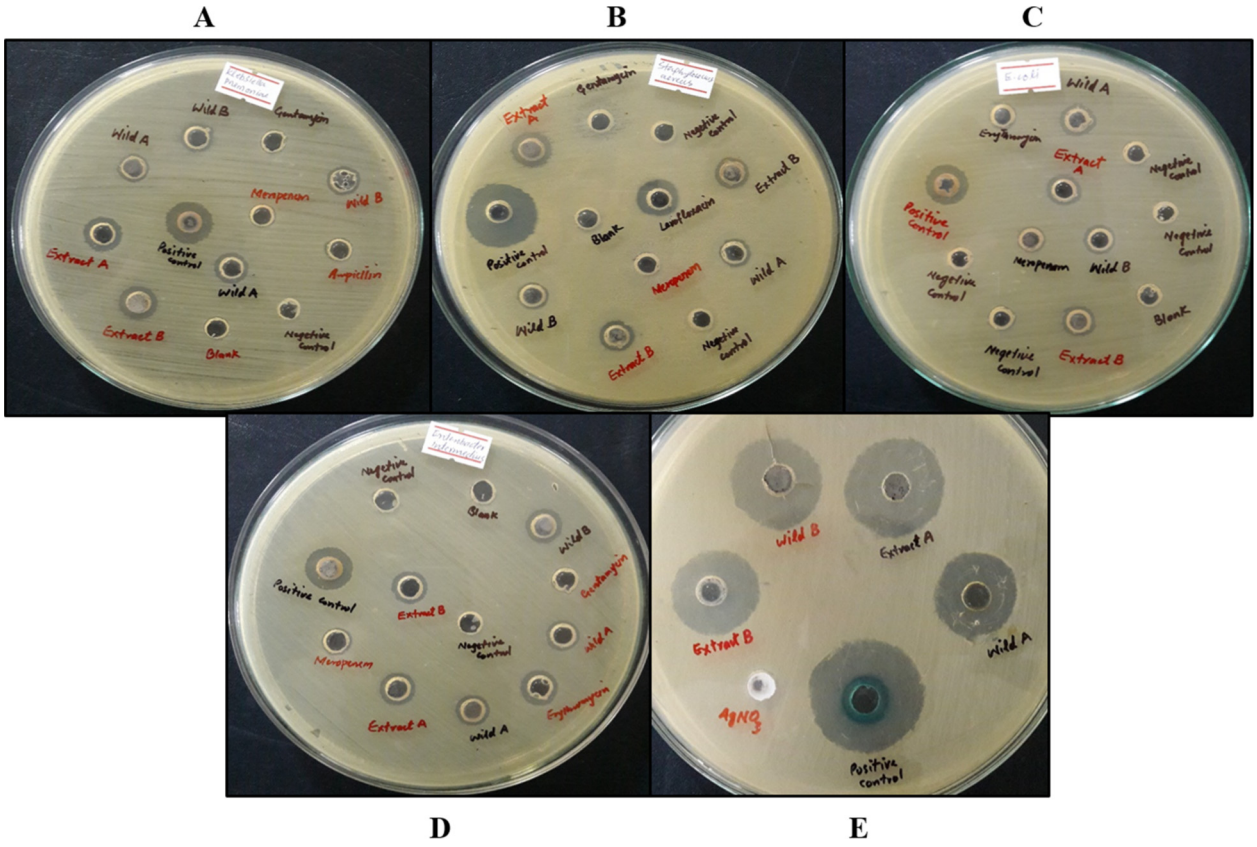

Fig. 8. Key: A (*Klebsiella pneumonia*), B (*Staphylococcus aureus*), C (*Escherichia coli*), D (*Enterobacter intermedius*), E (*Candid albicans*), Extract A = NPs, Extract B = extracts, Positive control = Ciprofloxacin (bacteria), Positive control = amphotericin B (fungi), Negative control = $AgNO_3$ salt, MDR strains (resistant to Erythromycin, Gentamycin, Meropenem, Ampicillin, Sensitive to Levofloxacin).

Table 5
Antibacterial and antifungal activity of NP1 (wild NPs), NP2 (wild extract), NP3 (seed NPs) and NP4 (seed extract).

(Diameter of zone of inhibition in mm)						
Bacterial, fungal strains	NP3	NP1	NP4	NP2	Positive control (ciprofloxacin 15 mg/mL, amphotericin B 10 mg/mL)	Negative control ($AgNO_3$ salt, 0.02 M)
Klebsiella pneumonia	6 mm	3 mm	6 mm	3 mm	10 mm	No zone
Staphylococcus aureus	5 mm	2 mm	3 mm	2 mm	15 mm	No zone
Escherichia coli	3 mm	4 mm	3 mm	2 mm	10 mm	No zone
Enterobacter intermedius	5 mm	5 mm	4 mm	5 mm	10 mm	No zone
Candida albicans	13 mm	10 mm	12 mm	10 mm	18 mm	No zone

(a class III deacetylase) has emerged as longevity key factor that control effects of oxidative stress antioxidant response stimulation through p53 and FOXOS pathways [85]. SIRT-1 activity stimulation has been reported to be vital in the process of regulation of aging and oxidative stress control [86,87]. The phytochemicals have been reported to prolong life span in *Caenorhabditis elegans* models, drosophila, and yeast and to activate SIRT-1 homologs [88,89].

The results of our test samples are shown in Table 3, as % of relative activities compare to control (consisting in assay and extraction solvent). The highest inhibition activity was shown by NP4 (48.89 ± 1.34) and NP2 (47.64 ± 1.67) against Pentosidine-like AGEs respectively followed by NP4 (44.46 ± 1.12) and NP2 (41.95 ± 1.09) against Vesperlysine-like AGEs, respectively. The rest of the activity is shown in Table 3. Our results match with previous studies [90,91].

5.4. Anti-diabetic activities

Around the world the major causes of morbidity and mortality is diabetes and related complications [92]. To study the anti-diabetic potential of *Silybum* extracts and NPs, two enzymatic assays i.e., α-glucosidase and solubilized α-amylase inhibition, were performed (shown in % inhibition activity). The highest anti-diabetic activity was shown by NP4 (38.74%) followed by NP2 (38.42%). Overall the extracts samples have more anti-diabetic activity as shown in the Table 4. Our results are in harmony with previous reports [93,94].

5.5. Cytotoxic screening

The cytotoxicity/antiproliferative was evaluated using MTT assay of the synthesized NPs and extracts (20 mg/mL stock in water) against HepG2 cell lines. It is clear from the results that cytotoxicity was shown by all the extracts and NPs towards non-treated HepG2 cells. The non-treated cells (NTCs) % viability was observed to be 100 ± 5.2% of viable cells, which dropped to 68.5 ± 2.0% in NP4 extract presence. Maximum cytotoxic/antiproliferative effect was seen at 100 μg/mL dose in the presence of NP2, NP3 and NP1 (52.4 ± 1.3%, 54.8 ± 0.9%, and 55.1 ± 0.7% of viable cells respectively)

(Fig. 7A).The lower the sample values, the more the effective are against liver cancer cells. Our results match with previous reports [95,96].

5.6. Antibacterial and antifungal activities

NP3, NP1, NP4 and NP2 have significant antibacterial and antifungal activity against several multi-drug resistant human pathogens like *Klebsiella pneumonia*, *Staphylococcus aureus*, *Escherichia coli*, *Enterobacter intermedius* and *Candida albicans*. Table 6 describes the antibacterial and antifungal potential of NP3, NP1, NP4 and NP2 against MDR human pathogens. NP3, NP1, NP4 and NP2 gave 6 mm, 3 mm, 6 mm and 3 mm zone of inhibition respectively in plate streaked with *Klebsiella pneumonia*. Plate containing *Staphylococcus aureus* gave 5 mm, 2 mm, 3 mm and 2 mm zone of inhibition against NP3, NP1, NP4 and NP2, respectively. Activity of NP3, NP1, NP4 and NP2 against *Escherichia coli* was 3 mm, 4 mm, 3 mm and 2 mm, respectively. NP3, NP1, NP4 and NP2 were also effective against *Enterobacter intermedius* and gave 5 mm, 5 mm, 4 mm and 5 mm of zone inhibition, respectively. Antifungal activity of NP3, NP1, NP4 and NP2 against *Candida albicans* was significantly high in comparison to antibacterial potential and zone of inhibition were 13 mm, 10 mm, 12 mm and 10 mm determined respectively (Fig. 8). Current antibacterial and antifungal results exhibited that NP3, NP1, NP4 and NP2 have considerable antibacterial and antifungal efficacy. The activity showed that gram negative bacteria were more prone to growth inhibition than gram positive bacteria and activity was maximum against fungi. It is suggested that antibacterial and antifungal activity may be due to microbial cell membrane perforation or due to the action of reactive oxygen species (ROS), generated by NP3, NP1, NP4 and NP2 [97]. These NPs can also actively penetrate the cell membrane through small pores in the microbial cell membrane and may cause the imbalance of minerals and leakage of intracellular proteins and enzymes, resulting in cell growth inhibition and death. [98]. The antimicrobial activity of silver is higher than copper, mercury, tin, chromium and lead [99]. The silver and its ions antibacterial mechanism involve the interaction of thiol groups of proteins molecules present outside or inside the cell membrane and binds the cell membrane of bacteria which inhibit replication of DNA molecule, thus affecting the viability of cell [100,101]. The AgNPs exhibit improve antibacterial activity due high fraction of surface atoms and high surface area, which lead to incorporate more NPs inside bacteria and promote its efficacy in a sustain manner [102,103]. Our results are similar to previous results [104,105]. (See Table 5.)

6. Conclusions

In the current era NPs are the tools for research in almost every field due to their extensive applications. NPs are most widely applicable in the field of medical sciences therefore; our research involves manipulation of green synthesized NPs from seeds and wild *Silybum marianum* with their respective extracts as cytotoxic against cancer cells, anti-oxidants, anti-inflammatory, anti-aging, anti-bacterial and anti-diabetic agents. For the current study the synthesis of silver NPs were selected due to efficient protocol and bio-compatible nature. The synthesized NPs and their respective extracts showed potent biological activities. The highest anti-oxidant activity was shown by NP4 and NP2 respectively. While the highest anti-fungal and antibacterial activities were shown by NP3 and NP4, respectively. Similarly high value of Pentosidine-Like AGEs and anti-diabetic was shown by NP4. The extracts and the green synthesized NPs could be suitable candidates for various biomedical research and applications.

Ethical approval

The study was approved by the Bioethical committee of Quaid-i-Azam University, Islamabad, Pakistan.

CRediT authorship contribution statement

Muzamil Shah: Conceptualization, Methodology, Software. **Sabir Nawaz:** Data curation, Writing - original draft. **Hasnain Jan:** Data curation, Writing - original draft. **Noor Uddin:** Visualization, Investigation. **Ashaq Ali:** Visualization, Investigation. **Sumaira Anjum:** Writing - review & editing. **Nathalie Giglioli-Guivarc'h:** Software, Validation. **Christophe Hano:** Software, Validation, Writing - review & editing. **Bilal Haider Abbasi:** Supervision, Writing - review & editing.

Declaration of competing interest

The authors declare that they have no known competing financial interests or personal relationships that could have appeared to influence the work reported in this paper.

References

[1] M. Fakruddin, Z. Hossain, H. Afroz, Prospects and applications of nanobiotechnology: a medical perspective, Journal of nanobiotechnology 10 (1) (2012) 31.
[2] L. Mazzola, Commercializing nanotechnology, Nat. Biotechnol. 21 (10) (2003) 1137.
[3] S. Kaviya, J. Santhanalakshmi, B. Viswanathan, Green synthesis of silver nanoparticles using Polyalthia longifolia leaf extract along with D-sorbitol: study of antibacterial activity, Journal of nanotechnology 2011 (2011).
[4] T. Vinod, R. Jelinek, Inorganic nanoparticles in cosmetics, Nanocosmetics, Springer, 2019, pp. 29–46.
[5] W. Muhammad, et al., *Papaver somniferum* L. mediated novel bioinspired lead oxide (PbO) and iron oxide (Fe_2O_3) nanoparticles: in-vitro biological applications, biocompatibility and their potential towards HepG2 cell line, Mater. Sci. Eng. C 103 (2019) 109740.
[6] R.J. Peters, et al., Nanomaterials for products and application in agriculture, feed and food, Trends Food Sci. Technol. 54 (2016) 155–164.
[7] A. Mondal, N.R. Jana, Graphene-nanoparticle composites and their applications in energy, environmental and biomedical science, Reviews in Nanoscience and Nanotechnology 3 (3) (2014) 177–192.
[8] S. Busatto, et al., Organotropic drug delivery: synthetic nanoparticles and extracellular vesicles, Biomed. Microdevices 21 (2) (2019) 46.
[9] M.A. Ansari, et al., Applications of nanostructured polymer composites for gene delivery, Nanostructured Polymer Composites for Biomedical Applications, 2019, p. 211.
[10] N.C. Mueller, B. Nowack, Exposure modeling of engineered nanoparticles in the environment, Environmental science & technology 42 (12) (2008) 4447–4453.
[11] K.A. Khalil, et al., Preparation and characterization of electrospun PLGA/silver composite nanofibers for biomedical applications, Int. J. Electrochem. Sci. 8 (3) (2013) 3483–3493.
[12] Z. Khan, et al., Preparation and characterization of silver nanoparticles by chemical reduction method, Colloids Surf. B: Biointerfaces 82 (2) (2011) 513–517.
[13] G. Singhal, et al., Biosynthesis of silver nanoparticles using *Ocimum sanctum* (Tulsi) leaf extract and screening its antimicrobial activity, J. Nanopart. Res. 13 (7) (2011) 2981–2988.
[14] S. Prabhu, E.K. Poulose, Silver nanoparticles: mechanism of antimicrobial action, synthesis, medical applications, and toxicity effects, International nano letters 2 (1) (2012) 32.
[15] H. Jiang, et al., Plasma-enhanced deposition of silver nanoparticles onto polymer and metal surfaces for the generation of antimicrobial characteristics, J. Appl. Polym. Sci. 93 (3) (2004) 1411–1422.
[16] G. Nam, et al., Investigating the versatility of multifunctional silver nanoparticles: preparation and inspection of their potential as wound treatment agents, International Nano Letters 6 (1) (2016) 51–63.
[17] S. Ahmed, et al., A review on plants extract mediated synthesis of silver nanoparticles for antimicrobial applications: a green expertise, J. Adv. Res. 7 (1) (2016) 17–28.
[18] S.S. Shankar, et al., Controlling the optical properties of lemongrass extract synthesized gold nanotriangles and potential application in infrared-absorbing optical coatings, Chem. Mater. 17 (3) (2005) 566–572.
[19] A. Panáček, et al., Antifungal activity of silver nanoparticles against *Candida* spp, Biomaterials 30 (31) (2009) 6333–6340.
[20] N. Durán, et al., Mechanistic aspects of biosynthesis of silver nanoparticles by several Fusarium oxysporum strains, Journal of nanobiotechnology 3 (1) (2005) 8.
[21] S. Silver, Bacterial silver resistance: molecular biology and uses and misuses of silver compounds, FEMS Microbiol. Rev. 27 (2–3) (2003) 341–353.
[22] T. Klaus, et al., Silver-based crystalline nanoparticles, microbially fabricated, Proc. Natl. Acad. Sci. 96 (24) (1999) 13611–13614.
[23] K. Zodrow, et al., Polysulfone ultrafiltration membranes impregnated with silver nanoparticles show improved biofouling resistance and virus removal, Water Res. 43 (3) (2009) 715–723.
[24] D. Mohale, et al., A pharmacological review on cyclooxygenase enzyme, Ind. J. Pharm. Pharmacol 1 (1) (2014) 46–58.

[25] W. Qing, et al., Functionalization of silver nanoparticles with mPEGylated luteolin for selective visual detection of Hg^{2+} in water sample, RSC Adv. 8 (51) (2018) 28843–28846.
[26] D. Tungmunnithum, et al., Flavonoids and other phenolic compounds from medicinal plants for pharmaceutical and medical aspects: an overview, Medicines 5 (3) (2018) 93.
[27] L. Abenavoli, et al., Milk thistle (*Silybum marianum*): a concise overview on its chemistry, pharmacological, and nutraceutical uses in liver diseases, Phytother. Res. 32 (11) (2018) 2202–2213.
[28] A. Borges, et al., COX inhibition profiles and molecular docking studies of the lignan hinokinin and some synthetic derivatives, Molecular Informatics 37 (12) (2018) 1800037.
[29] B.H. Abbasi, et al., *Isodon rugosus* (Wall. ex Benth.) codd in vitro cultures: establishment, phytochemical characterization and in vitro antioxidant and anti-aging activities, Int. J. Mol. Sci. 20 (2) (2019) 452.
[30] D. Coricovac, et al., Assessment of the effects induced by two triterpenoids on liver mitochondria respiratory function isolated from aged rats, Rev. Chim. 66 (2015) 1707–1710.
[31] A.W. Boots, G.R. Haenen, A. Bast, Health effects of quercetin: from antioxidant to nutraceutical, Eur. J. Pharmacol. 585 (2–3) (2008) 325–337.
[32] D.J. Kroll, H.S. Shaw, N.H. Oberlies, Milk thistle nomenclature: why it matters in cancer research and pharmacokinetic studies, Integrative cancer therapies 6 (2) (2007) 110–119.
[33] D. Jain, et al., Synthesis of plant-mediated silver nanoparticles using papaya fruit extract and evaluation of their anti microbial activities, Digest journal of nanomaterials and biostructures 4 (3) (2009) 557–563.
[34] P. Purushoth, R. Suresh, S. Selvakumari, Phytochemical analysis of ethanolic extract of *Merremia emaraginata* Burm, F by GC-MS. RJBCPS 10 (3) (2012).
[35] J.-W. Wu, L.-C. Lin, T.-H. Tsai, Drug–drug interactions of silymarin on the perspective of pharmacokinetics, J. Ethnopharmacol. 121 (2) (2009) 185–193.
[36] R. Lopez, et al., Determination of minor and trace volatile compounds in wine by solid-phase extraction and gas chromatography with mass spectrometric detection, J. Chromatogr. A 966 (1–2) (2002) 167–177.
[37] M. Shah, et al., Interactive effects of light and melatonin on biosynthesis of silymarin and anti-inflammatory potential in callus cultures of *Silybum marianum* (L.) Gaertn, Molecules 24 (7) (2019) 1207.
[38] B. Mozetič, P. Trebše, J. Hribar, Determination and quantitation of anthocyanins and hydroxycinnamic acids in different cultivars of sweet cherries (*Prunus avium* L.) from Nova Gorica region (Slovenia), Food Technol. Biotechnol. 40 (3) (2002) 207–212.
[39] C. Hano, et al., Flaxseed (*Linum usitatissimum* L.) extract as well as (+)-secoisolariciresinol diglucoside and its mammalian derivatives are potent inhibitors of α-amylase activity, Bioorg. Med. Chem. Lett. 23 (10) (2013) 3007–3012.
[40] Y. Velioglu, et al., Antioxidant activity and total phenolics in selected fruits, vegetables, and grain products, J. Agric. Food Chem. 46 (10) (1998) 4113–4117.
[42] B.H. Abbasi, et al., Shoot regeneration and free-radical scavenging activity in Silybum marianum L, Plant Cell, Tissue and Organ Culture (PCTOC) 101 (3) (2010) 371–376.
[43] M. Ahmed, et al., Polarity directed optimization of phytochemical and in vitro biological potential of an indigenous folklore: Quercus dilatata Lindl. ex Royle, BMC Complement. Altern. Med. 17 (1) (2017) 386.
[44] H. Fatima, et al., Extraction optimization of medicinally important metabolites from *Datura innoxia* Mill.: an in vitro biological and phytochemical investigation, BMC Complement. Altern. Med. 15 (1) (2015) 376.
[45] J. Wittenauer, et al., Inhibitory effects of polyphenols from grape pomace extract on collagenase and elastase activity, Fitoterapia 101 (2015) 179–187.
[46] P. Kolakul, B. Sripanidkulchai, Phytochemicals and anti-aging potentials of the extracts from *Lagerstroemia speciosa* and *Lagerstroemia floribunda*, Ind. Crop. Prod. 109 (2017) 707–716.
[47] W.-M. Chai, et al., Condensed tannins from longan bark as inhibitor of tyrosinase: structure, activity, and mechanism, J. Agric. Food Chem. 66 (4) (2018) 908–917.
[48] N. Kaewseejan, S. Siriamornpun, Bioactive components and properties of ethanolic extract and its fractions from *Gynura procumbens* leaves, Ind. Crop. Prod. 74 (2015) 271–278.
[49] M.R. Eftink, C.A. Ghiron, Fluorescence quenching studies with proteins, Anal. Biochem. 114 (2) (1981) 199–227.
[50] A.M. Fayaz, et al., Biogenic synthesis of silver nanoparticles and their synergistic effect with antibiotics: a study against gram-positive and gram-negative bacteria, Nanomedicine 6 (1) (2010) 103–109.
[51] R. Desai, et al., Size distribution of silver nanoparticles: UV–visible spectroscopic assessment, Nanosci. Nanotechnol. Lett. 4 (1) (2012) 30–34.
[52] B.H. Abbasi, et al., Biogenic synthesis of Au, Ag and Au–Ag alloy nanoparticles using Cannabis sativa leaf extract, IET Nanobiotechnology 12 (3) (2017) 277–284.
[53] B.H. Abbasi, et al., A comparative evaluation of the antiproliferative activity against HepG2 liver carcinoma cells of plant-derived silver nanoparticles from basil extracts with contrasting anthocyanin contents, Biomolecules 9 (8) (2019) 320.
[54] Malathi, R. and V. Ganesan, International Journal of Pharmaceutical Research and Bio-science.
[55] K. Shameli, et al., Green biosynthesis of silver nanoparticles using *Callicarpa maingayi* stem bark extraction, Molecules 17 (7) (2012) 8506–8517.
[56] K. Mallikarjuna, et al., Green synthesis of silver nanoparticles using *Ocimum* leaf extract and their characterization, Digest Journal of Nanomaterials and Biostructures 6 (1) (2011) 181–186.
[57] R. Gopalakrishnan, K. Raghu, Biosynthesis and characterization of gold and silver nanoparticles using milk thistle (*Silybum marianum*) seed extract, Journal of Nanoscience (2014), https://doi.org/10.1155/2014/905404.
[58] A.K. Jha, K. Prasad, Green synthesis of silver nanoparticles using *Cycas* leaf, International Journal of Green Nanotechnology: Physics and Chemistry 1 (2) (2010) P110–P117.
[59] N. Ahmad, et al., Rapid synthesis of silver nanoparticles using dried medicinal plant of basil, Colloids Surf. B: Biointerfaces 81 (1) (2010) 81–86.
[60] J.S. Kim, et al., Antimicrobial effects of silver nanoparticles, Nanomedicine 3 (1) (2007) 95–101.
[61] R. Mohammadinejad, et al., Synthesis of silver nanoparticles using *Silybum marianum* seed extract, International Journal of Nanoscience and Nanotechnology 9 (4) (2013) 221–226.
[62] D. Molins-Delgado, et al., On-line solid phase extraction-liquid chromatography-tandem mass spectrometry for insect repellent residue analysis in surface waters using atmospheric pressure photoionization, J. Chromatogr. A 1544 (2018) 33–40.
[63] Z. Li, et al., Synthesis and application of surface-imprinted activated carbon sorbent for solid-phase extraction and determination of copper (II), Spectrochim. Acta A Mol. Biomol. Spectrosc. 117 (2014) 422–427.
[64] S.M. Dehaghi, et al., Removal of permethrin pesticide from water by chitosan–zinc oxide nanoparticles composite as an adsorbent, Journal of Saudi Chemical Society 18 (4) (2014) 348–355.
[65] S. Drouet, et al., Single laboratory validation of a quantitative core shell-based LC separation for the evaluation of silymarin variability and associated antioxidant activity of pakistani ecotypes of milk thistle (*Silybum marianum* L.), Molecules 23 (4) (2018) 904.
[66] M.S. Abdel-Aziz, et al., Antioxidant and antibacterial activity of silver nanoparticles biosynthesized using *Chenopodium murale* leaf extract, Journal of Saudi Chemical Society 18 (4) (2014) 356–363.
[67] G. Karimi, et al., "Silymarin", a promising pharmacological agent for treatment of diseases, Iranian journal of basic medical sciences 14 (4) (2011) 308.
[68] J. Feher, G. Lengyel, Silymarin in the prevention and treatment of liver diseases and primary liver cancer, Curr. Pharm. Biotechnol. 13 (1) (2012) 210–217.
[69] V. Alexieva, et al., The effect of drought and ultraviolet radiation on growth and stress markers in pea and wheat, Plant Cell Environ. 24 (12) (2001) 1337–1344.
[70] N.A. Ashry, H.I. Mohamed, Impact of secondary metabolites and related enzymes in flax resistance and or susceptibility to powdery mildew, World J. Agric. Sci 7 (1) (2011) 78–85.
[71] G. Samuolienė, et al., The effect of red and blue light component on the growth and development of frigo strawberries, Zemdirbyste-Agriculture 97 (2) (2010) 99–104.
[72] N.J. Reddy, et al., Evaluation of antioxidant, antibacterial and cytotoxic effects of green synthesized silver nanoparticles by Piper longum fruit, Mater. Sci. Eng. C 34 (2014) 115–122.
[73] M.K. Swamy, et al., The green synthesis, characterization, and evaluation of the biological activities of silver nanoparticles synthesized from Leptadenia reticulata leaf extract, Appl. Nanosci. 5 (1) (2015) 73–81.
[74] D.-O. Kim, et al., Quantification of polyphenolics and their antioxidant capacity in fresh plums, J. Agric. Food Chem. 51 (22) (2003) 6509–6515.
[75] S. Aghazadeh, et al., Anti-apoptotic and anti-inflammatory effects of *Silybum marianum* in treatment of experimental steatohepatitis, Exp. Toxicol. Pathol. 63 (6) (2011) 569–574.
[76] E. Shaker, H. Mahmoud, S. Mnaa, Silymarin, the antioxidant component and *Silybum marianum* extracts prevent liver damage, Food Chem. Toxicol. 48 (3) (2010) 803–806.
[77] S. Pradhan, C. Girish, Hepatoprotective herbal drug, silymarin from experimental pharmacology to clinical medicine, Indian J. Med. Res. 124 (5) (2006) 491–504.
[78] L.Y. Guo, et al., Anti-inflammatory effects of schisandrin isolated from the fruit of *Schisandra chinensis* Baill, Eur. J. Pharmacol. 591 (1–3) (2008) 293–299.
[79] Z.X. Lim, A.P.K. Ling, S. Hussein, Callus induction of *Ocimum sanctum* and estimation of its total flavonoids content, Asian Journal of Agricultural Sciences 1 (2) (2009) 55–61.
[80] G.D. Liyanaarachchi, et al., Tyrosinase, elastase, hyaluronidase, inhibitory and antioxidant activity of Sri Lankan medicinal plants for novel cosmeceuticals, Ind. Crop. Prod. 111 (2018) 597–605.
[81] R. Boran, Investigations of anti-aging potential of *Hypericum origanifolium* Willd. for skincare formulations, Ind. Crop. Prod. 118 (2018) 290–295.
[82] T. Finkel, N.J. Holbrook, Oxidants, oxidative stress and the biology of ageing, nature 408 (6809) (2000) 239.
[83] P. Gkogkolou, M. Böhm, Advanced glycation end products: key players in skin aging? Dermato-endocrinology 4 (3) (2012) 259–270.
[84] D. Harraan, Aging: A Theory Based on Free Radical and Radiation Chemistry, (1955).
[85] Y.S. Hori, et al., Regulation of FOXOs and p53 by SIRT1 modulators under oxidative stress, PLoS One 8 (9) (2013) e73875.
[86] H.S. Ghosh, The anti-aging, metabolism potential of SIRT1, Current Opinion in Investigational Drugs (London, England: 2000) 9 (10) (2008) 1095–1102.
[87] M. Viswanathan, et al., A role for SIR-2.1 regulation of ER stress response genes in determining *C. elegans* life span, Dev. Cell 9 (5) (2005) 605–615.
[88] M. Viswanathan, L. Guarente, Regulation of *Caenorhabditis elegans* lifespan by sir-2.1 transgenes, Nature 477 (7365) (2011) E1.
[89] Y. He, et al., Green synthesis of silver nanoparticles by Chrysanthemum morifolium Ramat. Extract and their application in clinical ultrasound gel, Int. J. Nanomedicine 8 (2013) 1809.
[90] J.M. Ashraf, et al., Green synthesis of silver nanoparticles and characterization of their inhibitory effects on AGEs formation using biophysical techniques, Sci. Rep. 6 (2016) 20414.
[91] C. Jang, et al., Regulator of calcineurin 1 isoform 4 (RCAN1. 4) is overexpressed in

the glomeruli of diabetic mice, The Korean Journal of Physiology & Pharmacology 15 (5) (2011) 299–305.
[92] K. Rajaram, D. Aiswarya, P. Sureshkumar, Green synthesis of silver nanoparticle using *Tephrosia tinctoria* and its antidiabetic activity, Mater. Lett. 138 (2015) 251–254.
[93] N. Bala, et al., Green synthesis of zinc oxide nanoparticles using *Hibiscus subdariffa* leaf extract: effect of temperature on synthesis, anti-bacterial activity and anti-diabetic activity, RSC Adv. 5 (7) (2015) 4993–5003.
[94] K. Balan, et al., Antidiabetic activity of silver nanoparticles from green synthesis using *Lonicera japonica* leaf extract, RSC Adv. 6 (46) (2016) 40162–40168.
[95] G.M. Sulaiman, et al., Green synthesis, antimicrobial and cytotoxic effects of silver nanoparticles using *Eucalyptus chapmaniana* leaves extract, Asian Pac. J. Trop. Biomed. 3 (1) (2013) 58–63.
[96] A.E. Mohammed, Green synthesis, antimicrobial and cytotoxic effects of silver nanoparticles mediated by *Eucalyptus camaldulensis* leaf extract, Asian Pac. J. Trop. Biomed. 5 (5) (2015) 382–386.
[97] Q. Li, et al., Antimicrobial nanomaterials for water disinfection and microbial control: potential applications and implications, Water Res. 42 (18) (2008) 4591–4602.
[98] B. Reidy, et al., Mechanisms of silver nanoparticle release, transformation and toxicity: a critical review of current knowledge and recommendations for future studies and applications, Materials 6 (6) (2013) 2295–2350.
[99] S. Chen, G. Wu, H. Zeng, Preparation of high antimicrobial activity thiourea chitosan–Ag^{+} complex, Carbohydr. Polym. 60 (1) (2005) 33–38.
[100] W.K. Jung, et al., Antibacterial activity and mechanism of action of the silver ion in *Staphylococcus aureus* and *Escherichia coli*, Appl. Environ. Microbiol. 74 (7) (2008) 2171–2178.
[101] W.-R. Li, et al., Antibacterial activity and mechanism of silver nanoparticles on Escherichia coli, Appl. Microbiol. Biotechnol. 85 (4) (2010) 1115–1122.
[102] K.-H. Cho, et al., The study of antimicrobial activity and preservative effects of nanosilver ingredient, Electrochim. Acta 51 (5) (2005) 956–960.
[103] S. Bajpai, et al., Synthesis of polymer stabilized silver and gold nanostructures, J. Nanosci. Nanotechnol. 7 (9) (2007) 2994–3010.
[104] V. Kathiravan, et al., Green synthesis of silver nanoparticles using Croton sparsiflorus morong leaf extract and their antibacterial and antifungal activities, Spectrochim. Acta A Mol. Biomol. Spectrosc. 139 (2015) 200–205.
[105] W. Qing, et al., Cu^{2+}-doped carbon dots as fluorescence probe for specific recognition of Cr (VI) and its antimicrobial activity, Microchem. J. 152 (2020) 104262.